

# Multi-cause causal inference with unmeasured confounding and binary outcome

Dehan Kong

Department of Statistical Sciences, University of Toronto

Shu Yang

Department of Statistics, North Carolina State University

Linbo Wang

Department of Statistical Sciences, University of Toronto

for the Alzheimer's Disease Neuroimaging Initiative

## Abstract

Unobserved confounding presents a major threat to causal inference in observational studies. Recently, several authors suggest that this problem may be overcome in a shared confounding setting where multiple treatments are independent given a common latent confounder. It has been shown that if additional data such as negative controls are available, then the causal effects are indeed identifiable. In this paper, we show that these additional data are not necessary for causal identification, provided that the treatments and outcome follow Gaussian and logistic structural equation models, respectively. Our novel identification strategy is based on the symmetry and tail properties of the observed data distribution. We further develop two-step likelihood-based estimation procedures. We illustrate our method through simulations and a real data application studying the causal relationship between the volume of various brain regions and cognitive scores.

**Keywords:** Identifiability, Latent ignorability, Shared confounding

## 1 Introduction

Unmeasured confounding presents a major challenge to causal inference from observational studies. Without further assumptions, it is often impossible to identify the causal effects of interest. Classical approaches to mitigate bias due to unmeasured confounding include instrumental variable methods (e.g., Angrist et al., 1996; Hernán and Robins, 2006; Wang and Tchetgen Tchetgen, 2018), causal structure learning (e.g., Drton and Maathuis, 2017), invariant prediction (e.g., Peters et al., 2016), negative controls (e.g., Kuroki and Pearl, 2014; Miao et al., 2018) and sensitivity analysis (e.g., Cornfield et al., 1959).

In a recent stream of literature, several authors suggest an alternative approach to this problem by assuming shared confounding between multiple treatments and independence of treatments given the confounder (Wang and Blei, 2019a; Tran and Blei, 2017; Ranganath and Perotte, 2018; Wang and Blei, 2019b). This is a promising approach as it leverages information in a potentially high-dimensional treatment to aid causal identification. Such settings are prevalent in many contemporary applications such as genetics, recommendation systems and neuroimaging studies. Unfortunately, in general the shared confounding structure is not sufficient for causal identification. D’Amour (2019) presents two counterexamples: the first one involves normally-distributed treatments and outcome, and the second one involves binary treatments and outcome. To address this non-identifiability problem, D’Amour (2019) suggests applying classical ideas such as negative controls or sensitivity analysis to the shared confounding setting. Along this line, Wang and Blei (2019b) show that the deconfounder algorithm of Wang and Blei (2019a) is valid given a set of negative controls, and Veitch et al. (2019) further find a negative control in network settings.

In this paper, we show that identification of causal effects is possible under the shared confounding setting with normally-distributed treatments and a binary outcome following a logistic structural equation model. To the best of our knowledge, this result is the first in the literature that requires no external data but still identifies the causal effect in this setting. In contrast to the case with normally-distributed treatments and outcome, in general the observed data distribution may contain information beyond the first two moments, thereby providing many more non-trivial constraints for causal identification (Bentler, 1983; Bollen, 2014). In particular, we exploit the symmetry and tail properties of the observed data distribution to identify the causal effects. Our identification results are accompanied by simple likelihood-based estimation procedures, and illustrations through synthetic and real data analyses.

## 2 Framework

Let  $A = (A^1, A^2, \dots, A^p)^\top$  be a  $p$ -vector of continuous treatments,  $Y$  be an outcome and  $X$  be a  $q$ -vector of observed pre-treatment variables. The observed data  $\{(X_i, A_i, Y_i) : i = 1, \dots, n\}$  are independent samples from a super population. Under the potential outcome framework (Neyman, 1923; Rubin, 1974),  $Y(a)$  is the potential outcome if the patient had treatment  $a = (a^1, \dots, a^p)^\top$ . We are interested in the mean potential outcome  $E\{Y(a)\}$ . We make the stable unit treatment value assumption under which  $Y(a)$  is well-defined and  $Y = Y(a)$  if  $A = a$ .

We assume the shared confounding structure under which the latent ignorability assumption holds. Figure 1 provides a graphical illustration.

**Assumption 1 (Latent ignorability)** *For all  $a$ ,  $A \perp\!\!\!\perp Y(a) \mid (X, U)$ , where  $U$  is a latent confounder.*

Under Assumption 1, we have

$$E\{Y(a)\} = E\{E(Y \mid A = a, X, U)\}. \quad (1)$$

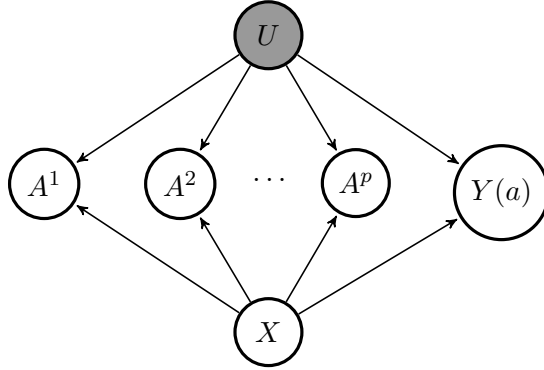


Figure 1: A graphical illustration of the shared confounding setting. The latent ignorability assumption is encoded by the absence of arrows between  $A^j$  and  $Y(a)$  for  $j = 1, \dots, p$ . The gray node denotes that  $U$  is unobserved.

Assuming a latent factor model for the treatments such as

$$U \sim \mathcal{N}(0, 1), \quad A = \theta U + \epsilon_A, \quad (2)$$

where  $\epsilon_A \sim \mathcal{N}(0, \text{diag}(\sigma_{A,1}^2, \dots, \sigma_{A,p}^2))$  and  $\epsilon_A \perp\!\!\!\perp U$ . Wang and Blei (2019a) suggest first constructing an estimate of  $U$ , the so-called de-confounder, and then use (1) to identify the mean potential outcome and causal contrasts. However, as pointed out by D’Amour (2019),  $E\{Y(a)\}$  is not necessarily identifiable. See also Example S1 in the supplementary materials for a counterexample where  $Y$  is generated from a Gaussian structural equation model.

### 3 Identification and estimation with a binary outcome

#### 3.1 Identification and estimation without observed confounders

We now study the identification and estimation problems with a binary  $Y$ , thereby operating under a different set of assumptions than Example S1. To fix ideas, we first consider the case without measured confounders  $X$  and later extend these results to the case with  $X$  in § 3.2. We assume that treatments  $A$  follow the factor model (2). We also assume the following logistic structural equation model:

$$\text{pr}\{Y(a) = 1 \mid U\} = \text{pr}\{Y = 1 \mid A = a, U\} = \text{expit}(\alpha + \beta^T a + \gamma U). \quad (3)$$

Since  $U$  is latent, without loss of generality, assume that  $\gamma \geq 0$ . Under (2), identifiability of  $E\{Y(a)\}$  amounts to identifiability of model parameters in (3).

We first note that under (2),  $(U, A^T)^T$  follows a joint multivariate normal distribution

$$\begin{pmatrix} U \\ A \end{pmatrix} \sim \mathcal{N}_{p+1}(0, \Sigma_J), \quad \Sigma_J = \begin{pmatrix} 1 & \theta^T \\ \theta & \Sigma_{AA} \end{pmatrix},$$

where  $\Sigma_{AA} = \theta\theta^T + \text{diag}(\sigma_{A,1}^2, \dots, \sigma_{A,p}^2)$ . Therefore,  $U|A = a$  follows a univariate normal distribution with mean  $\mu_{U|a} = \theta^T \Sigma_{AA}^{-1} a$  and variance  $\sigma_{U|a}^2 = 1 - \theta^T \Sigma_{AA}^{-1} \theta$ . Standard results from factor analysis (Anderson and Rubin, 1956) can be used to identify  $\Sigma_{AA}$ , and  $\theta$  up to a sign flip.

Our identification strategy is then based on the following equation that connects the observed distribution  $\text{pr}(Y = 1 | A = a)$  to the unknown structural distribution  $\text{pr}(Y = 1 | A = a, U = u)$ :

$$\begin{aligned} \text{pr}(Y = 1 | A = a; \alpha, \beta, \gamma, \theta, \Sigma_{AA}) &= \int \text{expit}(\alpha + \beta^T a + \gamma u) f_{U|A}(u|a) du \\ &= \int \text{expit}\{\alpha + (\beta^T + \gamma \theta^T \Sigma_{AA}^{-1}) a + \gamma \sigma_{U|a} v\} \phi(v) dv, \quad (4) \end{aligned}$$

where  $\phi(v)$  is the probability density function of a standard normal distribution. In the supplementary materials we show that under mild conditions, there is a bijection from the function  $Q(a) = \int \text{expit}(c_1 + c_2^T a + c_3 v) \phi(v) dv$  to its coefficients  $(c_1, c_2^T, c_3)$ . This result exploits several properties of the expit function, including its tail properties, monotonicity and symmetry around zero. It follows that one can identify  $\alpha, \beta$  and  $\gamma$  from (4).

We now present our main identification result, with the proof deferred to the supplementary materials.

**Theorem 1** *Assume that Assumption 1, models (2), (3) and the following conditions hold:*

- (A1) *There exist at least three elements of  $\theta = (\theta_1, \dots, \theta_p)^T$  that are non-zero, and there exists at least one  $\theta_j \neq 0$ ,  $1 \leq j \leq p$  such that the sign of  $\theta_j$  is known a priori.*
- (A2)  *$\text{pr}(Y = 1 | A = a)$  is not a constant function of  $a$ .*

*Then the parameters  $\theta, \Sigma_{AA}, \alpha, \beta, \gamma$  and hence  $E\{Y(a)\}$  are identifiable.*

Condition (A1) requires that the latent confounder  $U$  affects at least three treatments, and for at least one of which, subject-specific knowledge allows one to determine the sign of  $\theta_j$ . Condition (A2) requires that the observed mean outcomes differ across treatment levels, and can be checked from the observed data.

In parallel to our identification results, we develop a two-step estimation procedure to estimate the model parameters. Asymptotic normality and resulting inference procedures follow directly from standard M-estimation theory.

Step 1. Find the maximum likelihood estimator  $(\hat{\theta}, \hat{\Sigma}_{AA})^T$  using off-the-shelf packages for factor analysis, such as the `factanal` function in R.

Step 2. Find the maximum likelihood estimator  $(\hat{\alpha}, \hat{\beta}^T, \hat{\gamma})^T$  by maximizing the conditional likelihood  $\prod_{i=1}^n [r_i(\alpha, \beta, \gamma)^{Y_i} \{1 - r_i(\alpha, \beta, \gamma)\}^{1 - Y_i}]$ , where  $r_i(\alpha, \beta, \gamma) = \text{pr}(Y = 1 | A = A_i; \alpha, \beta, \gamma, \hat{\theta}, \hat{\Sigma}_{AA})$ . Monte Carlo method can be used to approximate the integral.

### 3.2 Incorporating observed confounders

In the presence of observed confounders  $X \in \mathbb{R}^q$ , we assume instead:

$$A = \theta U + BX + \epsilon_A, \quad (5)$$

$$\text{pr}\{Y(a) = 1 | U, X\} = \text{expit}(\alpha + \beta^T a + \gamma U + \eta^T X). \quad (6)$$

We also assume that  $(U, X, A)$  follows a multivariate normal distribution

$$\begin{pmatrix} U \\ X \\ A \end{pmatrix} \sim \mathcal{N}_{p+q+1}(0, \Sigma_J^*), \quad \Sigma_J^* = \begin{pmatrix} 1 & \Sigma_{UX} & \theta^T \\ \Sigma_{XU} & \Sigma_{XX} & \Sigma_{XA} \\ \theta & \Sigma_{AX} & \Sigma_{AA} \end{pmatrix}.$$

Since both  $U$  and  $\epsilon_A$  are latent, without loss of generality, let  $X \perp\!\!\!\perp (U, \epsilon_A)$  so that  $\Sigma_{UX} = 0$  and  $\Sigma_{AX} = B\Sigma_{XX}$ . If otherwise, one could project  $U$  to the orthogonal complement of the column space of  $X$ , to obtain  $U^* = (1 - P_X)U$  with  $P_X = X^T(XX^T)^{-1}X$ . It then holds that  $U^* \perp\!\!\!\perp X$ .

Let  $\tilde{\theta} = (0, \theta^T)^T \in \mathbb{R}^{p+q}$  and  $\tilde{\Sigma} = \begin{pmatrix} \Sigma_{XX} & \Sigma_{XX}B^T \\ B\Sigma_{XX} & \Sigma_{AA} \end{pmatrix}$ . Then  $U|X = x, A = a$  follows a univariate normal distribution with mean  $\mu_{U|x,a} = \tilde{\theta}^T \tilde{\Sigma}^{-1} (x^T, a^T)^T$  and variance  $\sigma_{U|x,a}^2 = 1 - \tilde{\theta}^T \tilde{\Sigma}^{-1} \tilde{\theta}$ . Similar to (4), we have

$$\begin{aligned} \text{pr}(Y = 1 | A = a, X = x) &= \int \text{expit}(\alpha + \beta^T a + \gamma u + \eta^T x) f_{U|A}(u|x, a) du \\ &= \int \text{expit}\{\alpha + (\tilde{\beta}^T + \gamma \tilde{\theta}^T \tilde{\Sigma}^{-1})(x^T, a^T)^T + \gamma \sigma_{U|x,a} v\} \phi(v) dv, \end{aligned}$$

where  $\tilde{\beta} = (\eta^T, \beta^T)^T$ . Identifiability of  $E\{Y(a)\}$  can then be obtained in a similar fashion as in § 3.1, except that now we replace condition (A2) with the following weaker assumption:

(A2\*)  $\text{pr}(Y = 1 | A = a, X = x)$  is not a constant function of  $(a, x)$

**Theorem 2** *Assume that Assumption 1, models (2), (3) and assumptions (A1), (A2\*) hold. Then the parameters  $\theta, \tilde{\Sigma}, \alpha, \eta, \beta, \gamma$  and hence  $E\{Y(a)\}$  are identifiable.*

A two-step estimation procedure proceeds as follows.

Step 1. For  $B$ , we regress  $A$  on  $X$  and obtain an estimator  $\hat{B} \in \mathbb{R}^{p \times q}$ . Let  $A^* = A - \hat{B}X$ , one can obtain the maximum likelihood estimator of  $\theta$  and  $\tilde{\Sigma}$  based on a factor analysis on  $A^*$ . Denote the estimator as  $\hat{\theta}$  and  $\hat{\tilde{\Sigma}}$ , respectively.

Step 2. Estimate  $(\alpha, \beta^T, \gamma, \eta)$  by maximizing the conditional likelihood  $\prod_{i=1}^n [r_{X,i}(\alpha, \beta, \gamma, \eta)^{Y_i} \{1 - r_{X,i}(\alpha, \beta, \gamma, \eta)\}^{1-Y_i}]$ , where  $r_{X,i}(\alpha, \beta, \gamma, \eta) = \text{pr}(Y = 1 | A = A_i, X = X_i; \alpha, \beta, \gamma, \eta, \hat{\theta}, \hat{\tilde{\Sigma}})$ .

## 4 Simulation

We now evaluate the finite sample performance of the proposed estimators. In our simulations, we first generate a latent confounder  $U$ , an observed common confounder  $X$  and an additional covariate  $X^1$  from independent standard normal distributions. The treatments and outcome are then generated from the following models:

$$A = \theta U + BX + B_1 X^1 + \epsilon_A,$$

$$\text{pr}(Y = 1|A, U, X, X^1) = \text{expit}(\alpha + \beta^T A + \gamma U + \eta X + \eta_1 X^1),$$

where  $\theta = (1, -1, 0.5)^T$ ,  $\alpha = 0$ ,  $\beta = (1, 1, 1)^T$ ,  $\gamma = 1$ , and  $\epsilon_A \sim \mathcal{N}_3(0, 0.25I_3)$ , where  $I_3$  denotes the  $3 \times 3$  identity matrix. We consider three settings. In setting 1, there are no observed confounders so that  $B = B_1 = (0, 0, 0)^T$ ,  $\eta = \eta_1 = 0$ . In setting 2, there is a common confounder  $X$  with  $B = (1, -1, 1)^T$ ,  $B_1 = (0, 0, 0)^T$ ,  $\eta = 1$ ,  $\eta_1 = 0$ . In setting 3, there is a common confounder  $X$  and a so-called single-cause confounder  $X^1$  with  $B = (1, -1, 1)^T$ ,  $B_1 = (1, 0, 0)^T$ ,  $\eta = \eta_1 = 1$ . We compare the proposed method, assuming that we know  $\theta_1 > 0$ , to a naive method where we only adjust for the observed confounders. Table 1 summarizes the results for sample size 200. Results with sample sizes 500 and 1000 are deferred to the supplementary materials.

Table 1: Simulation results for sample size 200 based on 1000 Monte Carlo samples: bias (standard deviation) of  $\hat{\beta}_1$ ,  $\hat{\beta}_2$ ,  $\hat{\beta}_3$  and the mean potential outcomes evaluated at  $a_{(1)} = (1, 1, 0)^T$  and  $a_{(2)} = (1, 1, 1)^T$ , are reported. In the naive method we fit the model ignoring the unobserved confounder  $U$

| Setting | Method   | $\hat{\beta}_1$ | $\hat{\beta}_2$ | $\hat{\beta}_3$ | $\hat{E}\{Y(a_{(1)})\}$ | $\hat{E}\{Y(a_{(2)})\}$ |
|---------|----------|-----------------|-----------------|-----------------|-------------------------|-------------------------|
| 1       | Proposed | 0.024(0.329)    | 0.019(0.303)    | 0.023(0.376)    | -0.006(0.069)           | -0.008(0.048)           |
|         | Naive    | -0.767(0.043)   | -0.899(0.046)   | -0.803(0.055)   | -0.148(0.018)           | -0.195(0.019)           |
| 2       | Proposed | 0.009(0.381)    | 0.015(0.370)    | 0.037(0.439)    | -0.013(0.079)           | -0.015(0.066)           |
|         | Naive    | -0.824(0.040)   | -0.926(0.042)   | -0.848(0.051)   | -0.139(0.017)           | -0.199(0.019)           |
| 3       | Proposed | 0.065(0.422)    | 0.034(0.424)    | 0.066(0.483)    | -0.009(0.09)            | -0.012(0.073)           |
|         | Naive    | -0.851(0.040)   | -0.937(0.039)   | -0.873(0.047)   | -0.126(0.017)           | -0.193(0.019)           |

One can see that the estimates obtained from the naive method is subject to unmeasured confounding bias. In contrast, the bias of our proposed estimator is small even for sample size 200, which further reduces as the sample size grows.

## 5 Real data application

Understanding how human brain works and their connection to human behavior is a central goal in neuroscience. Studies have found that neuroimaging markers are strongly associated with behavioral deficits

(Whitwell et al., 2007). For example, the atrophy of three regions in the brain, the temporal, cingulate cortex and hippocampal regions, are found to be strongly associated with symptoms of Alzheimer’s disease (Galton et al., 2001; Choo et al., 2010; Fox et al., 1996). These associations, however, may be confounded by common unmeasured factors such as progress of the underlying neuro-degenerative process. We now use the proposed approach to address bias due to common unmeasured confounding.

Our analysis is based on data from the Alzheimer’s Disease Neuroimaging Initiative. This is a large-scale observational study launched in 2003 through a \$60 million, 5-year public-private partnership between the National Institutes of Health, the Food and Drug Administration and several private pharmaceutical companies and non-profit organizations. The study recruited adults aged between 55 and 90 years old. The 800 participants include cognitively normal individuals, as well as subjects with mild cognitive impairments and early Alzheimer’s disease. For more details of the study, see [www.adni-info.org](http://www.adni-info.org).

In our analysis, the treatments  $A^1$ ,  $A^2$  and  $A^3$  are defined as the relative volume of three brain regions: the temporal, cingulate cortex and hippocampal regions; the relative volume is defined as the ratio between the volume of a specific brain region and the total volume of the brain. The outcome is an indicator that the Mini Mental State Examination score is smaller than 24, a measure of cognitive decline that has been commonly used in diagnosis of Alzheimer’s disease (O’Bryant et al., 2008). The observed confounders  $X$  include age and years of education. For illustrative purpose, we include 674 subjects with complete covariate information in our analysis. Among these subjects, the average age is 75.3 with a standard deviation of 6.8, and the average years of education is 15.7 with a standard deviation of 2.9. We assume that the treatments and outcome follow models (5) and (6), respectively. It is well-known that progress of the disease process contributes to both hippocampal atrophy and a lower Mini Mental State Examination score (Sabuncu et al., 2011), so that  $\theta_3 \leq 0$ .

Analysis results show that conditional on age, years of education and the latent disease progress, each one percent of shrinkage in the relative volume of the temporal, cingulate cortex and hippocampal regions causes the odds of developing a clinical relevant Alzheimer’s disease symptom, defined as the Mini Mental State Examination score being small than 24, to increase by 0.6% with 95% confidence interval [-1.1%, 2.3%], 1.4% with 95% confidence interval [-0.2%, 3.1%], 7.6% with 95% confidence interval [4.0%, 11.2%], respectively. The directions of causal effect estimates are consistent with associations reported in the literature, suggesting that the bias from latent confounding is not large enough to distort the qualitative causal conclusions. Our results show that shrinkage of the hippocampal region has a significant effect on the cognitive score, which aligns with the common belief that hippocampal atrophy is among the most significant structural biomarkers of Alzheimer’s disease imaging (Henneman et al., 2009).

We also compare the proposed and naive methods in terms of the mean potential outcomes. One can see from Figure 2 that compared to the proposed method, the naive method suggests a much weaker association between the shrinkage of brain regions and odds of developing Alzheimer’s disease, due to strong confounding by the latent disease progress.

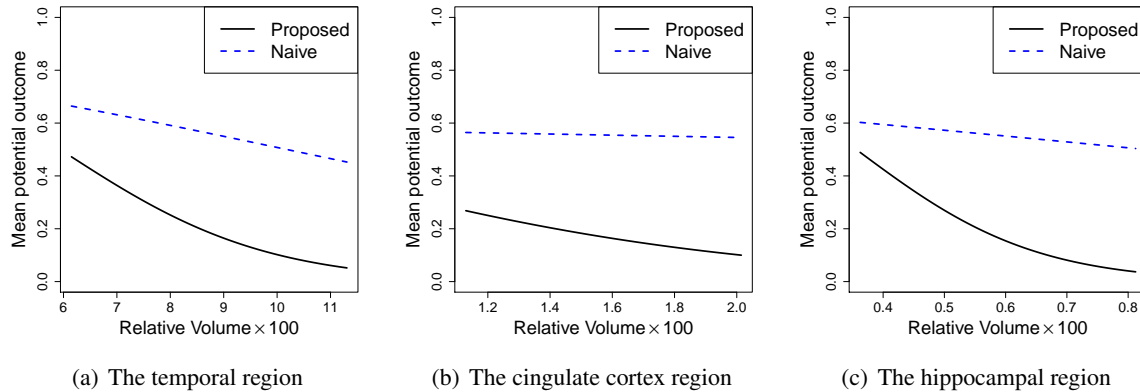


Figure 2: Estimated mean potential Alzheimer’s disease status as a function of the relative volume of three brain regions (in percentages). In each plot, the relative volume of the other two regions are fixed at their sample medians

## 6 Discussion

We have shown identifiability of causal effects under a shared confounding setting with a logistic structural equation model for the outcome. Interestingly, these identifiability results are not necessarily true with other structural equation models for a binary outcome. In particular, we have the following non-identifiability result for a probit model.

**Theorem 3** *Suppose that the outcome  $Y$  follows a probit structural equation model that*

$$\text{pr}\{Y(a) = 1 \mid U\} = \text{pr}(Y = 1 \mid A = a, U) = \Phi(\alpha + \beta^T a + \gamma U), \quad (7)$$

where  $\theta, \beta \in \mathbb{R}^p$ ,  $\epsilon_A \sim \mathcal{N}(0, \text{diag}(\sigma_{A,1}^2, \dots, \sigma_{A,p}^2))$  and  $\Phi(\cdot)$  is the cumulative density function of standard normal. Then under models (2) and (7), the parameters  $\alpha$ ,  $\beta$ ,  $\gamma$  and  $E\{Y(a)\}$  are not identifiable.

## References

- Anderson, T. W. and Rubin, H. (1956). Statistical inference in factor analysis. In *Proceedings of the third Berkeley symposium on mathematical statistics and probability*, volume 5, pages 111–150.
- Angrist, J. D., Imbens, G. W., and Rubin, D. B. (1996). Identification of causal effects using instrumental variables. *J. Am. Statist. Assoc.*, 91:444–455.
- Bentler, P. M. (1983). Simultaneous equation systems as moment structure models: With an introduction to latent variable models. *Journal of Econometrics*, 22(1-2):13–42.
- Bollen, K. A. (2014). *Structural equations with latent variables*, volume 210. John Wiley & Sons.



- Choo, I. H., Lee, D. Y., Oh, J. S., Lee, J. S., Lee, D. S., Song, I. C., Youn, J. C., Kim, S. G., Kim, K. W., Jhoo, J. H., et al. (2010). Posterior cingulate cortex atrophy and regional cingulum disruption in mild cognitive impairment and Alzheimer's disease. *Neurobiology of Aging*, 31(5):772–779.
- Cornfield, J., Haenszel, W., Hammond, E. C., Lilienfeld, A. M., Shimkin, M. B., and Wynder, E. L. (1959). Smoking and lung cancer: recent evidence and a discussion of some questions. *Journal of the National Cancer Institute*, 22(1):173–203.
- D'Amour, A. (2019). On multi-cause approaches to causal inference with unobserved confounding: Two cautionary failure cases and a promising alternative. In *The 22nd International Conference on Artificial Intelligence and Statistics*, pages 3478–3486.
- Drton, M. and Maathuis, M. H. (2017). Structure learning in graphical modeling. *Annual Review of Statistics and Its Application*, 4:365–393.
- Fox, N., Warrington, E., Freeborough, P., Hartikainen, P., Kennedy, A., Stevens, J., and Rossor, M. N. (1996). Presymptomatic hippocampal atrophy in Alzheimer's disease: A longitudinal MRI study. *Brain*, 119(6):2001–2007.
- Galton, C. J., Patterson, K., Graham, K., Lambon-Ralph, M. A., Williams, G., Antoun, N., Sahakian, B., and Hodges, J. (2001). Differing patterns of temporal atrophy in Alzheimer's disease and semantic dementia. *Neurology*, 57(2):216–225.
- Henneman, W., Sluimer, J., Barnes, J., Van Der Flier, W., Sluimer, I., Fox, N., Scheltens, P., Vrenken, H., and Barkhof, F. (2009). Hippocampal atrophy rates in alzheimer disease: added value over whole brain volume measures. *Neurology*, 72(11):999–1007.
- Hernán, M. A. and Robins, J. M. (2006). Instruments for causal inference: An epidemiologist's dream? *Epidemiology*, 17(4):360–372.
- Kuroki, M. and Pearl, J. (2014). Measurement bias and effect restoration in causal inference. *Biometrika*, 101(2):423–437.
- Miao, W., Geng, Z., and Tchetgen Tchetgen, E. J. (2018). Identifying causal effects with proxy variables of an unmeasured confounder. *Biometrika*, 105(4):987–993.
- Neyman, J. (1923). Sur les applications de la thar des probabilités aux expériences Agaricales: Essay des principe. English translation of excerpts by Dabrowska, D. and Speed, T. (1990). *Statist. Sci.*, 5:463–472.
- O'Bryant, S. E., Humphreys, J. D., Smith, G. E., Ivnik, R. J., Graff-Radford, N. R., Petersen, R. C., and Lucas, J. A. (2008). Detecting dementia with the mini-mental state examination in highly educated individuals. *Archives of Neurology*, 65(7):963–967.

- Peters, J., Bühlmann, P., and Meinshausen, N. (2016). Causal inference by using invariant prediction: identification and confidence intervals. *J. R. Stat. Soc. Ser. B.*, 78(5):947–1012.
- Ranganath, R. and Perotte, A. (2018). Multiple causal inference with latent confounding. *arXiv preprint arXiv:1805.08273*.
- Rubin, D. B. (1974). Estimating causal effects of treatments in randomized and nonrandomized studies. *Journal of Educational Psychology*, 66(5):688.
- Sabuncu, M. R., Desikan, R. S., Sepulcre, J., Yeo, B. T. T., Liu, H., Schmansky, N. J., Reuter, M., Weiner, M. W., Buckner, R. L., Sperling, R. A., et al. (2011). The dynamics of cortical and hippocampal atrophy in alzheimer disease. *Archives of neurology*, 68(8):1040–1048.
- Tran, D. and Blei, D. M. (2017). Implicit causal models for genome-wide association studies. *arXiv preprint arXiv:1710.10742*.
- Veitch, V., Wang, Y., and Blei, D. M. (2019). Using embeddings to correct for unobserved confounding. *arXiv preprint arXiv:1902.04114*.
- Wang, L. and Tchetgen Tchetgen, E. (2018). Bounded, efficient and multiply robust estimation of average treatment effects using instrumental variables. *J. R. Stat. Soc. Ser. B.*, 80:531–550.
- Wang, Y. and Blei, D. M. (2019a). The blessings of multiple causes. *J. Am. Statist. Assoc. (with discussion)*, (just-accepted).
- Wang, Y. and Blei, D. M. (2019b). Multiple causes: A causal graphical view. *arXiv preprint arXiv:1905.12793*.
- Whitwell, J. L., Weigand, S. D., Shiung, M. M., Boeve, B. F., Ferman, T. J., Smith, G. E., Knopman, D. S., Petersen, R. C., Benarroch, E. E., Josephs, K. A., et al. (2007). Focal atrophy in dementia with lewy bodies on MRI: a distinct pattern from Alzheimer’s disease. *Brain*, 130(3):708–719.

# Supplementary materials for “Multi-cause causal inference with unmeasured confounding and binary outcome”

Dehan Kong, Shu Yang and Linbo Wang

## 1 Additional simulation results

In this section, we include additional simulation results. In particular, we include the simulation results with  $n = 500$  and  $n = 1000$  in Tables S1.

Table S1: Simulation results based on 1000 Monte Carlo samples: bias (standard deviation) of  $\hat{\beta}_1$ ,  $\hat{\beta}_2$ ,  $\hat{\beta}_3$  and the mean potential outcomes evaluated at  $a_{(1)} = (1, 1, 0)^T$  and  $a_{(2)} = (1, 1, 1)^T$ , are reported. In the naive method we fit the model ignoring the unobserved confounder  $U$

| Setting            | Method   | $\hat{\beta}_1$ | $\hat{\beta}_2$ | $\hat{\beta}_3$ | $\hat{E}\{Y(a_{(1)})\}$ | $\hat{E}\{Y(a_{(2)})\}$ |
|--------------------|----------|-----------------|-----------------|-----------------|-------------------------|-------------------------|
| Sample size = 500  |          |                 |                 |                 |                         |                         |
| 1                  | Proposed | -0.007(0.204)   | -0.004(0.192)   | -0.002(0.236)   | -0.005(0.045)           | -0.005(0.030)           |
|                    | Naive    | -0.770(0.027)   | -0.902(0.029)   | -0.803(0.035)   | -0.149(0.012)           | -0.195(0.012)           |
| 2                  | Proposed | 0.002(0.227)    | 0.001(0.224)    | -0.013(0.246)   | -0.005(0.050)           | -0.007(0.038)           |
|                    | Naive    | -0.823(0.025)   | -0.924(0.026)   | -0.851(0.031)   | -0.138(0.011)           | -0.198(0.012)           |
| 3                  | Proposed | 0.021(0.253)    | 0.011(0.252)    | 0.029(0.287)    | -0.006(0.058)           | -0.006(0.045)           |
|                    | Naive    | -0.850(0.025)   | -0.935(0.024)   | -0.872(0.031)   | -0.126(0.011)           | -0.192(0.012)           |
| Sample size = 1000 |          |                 |                 |                 |                         |                         |
| 1                  | Proposed | -0.010(0.142)   | -0.001(0.130)   | -0.016(0.160)   | -0.003(0.030)           | -0.004(0.020)           |
|                    | Naive    | -0.769(0.019)   | -0.901(0.020)   | -0.803(0.024)   | -0.149(0.008)           | -0.195(0.008)           |
| 2                  | Proposed | -0.009(0.171)   | 0.006(0.158)    | 0.000(0.174)    | -0.004(0.037)           | -0.004(0.028)           |
|                    | Naive    | -0.823(0.018)   | -0.924(0.018)   | -0.848(0.022)   | -0.138(0.008)           | -0.198(0.008)           |
| 3                  | Proposed | -0.003(0.172)   | 0.008(0.171)    | 0.003(0.188)    | -0.005(0.041)           | -0.005(0.033)           |
|                    | Naive    | -0.851(0.017)   | -0.936(0.018)   | -0.871(0.021)   | -0.126(0.007)           | -0.192(0.008)           |

## 2 A Counterexample

**Example S1** Assume model (2) and the following model

$$Y(a) = \beta^T a + \gamma U + \epsilon_Y, \tag{S1}$$

where  $\beta = (\beta_1, \dots, \beta_p)^\top \in \mathbb{R}^p$ ,  $\epsilon_Y \sim \mathcal{N}(0, \sigma_Y^2)$  and  $\epsilon_Y \perp\!\!\!\perp (A, U)$ . Under models (2) and (S1),  $E\{Y(a)\} = E\{E(Y|A = a, U)\} = \beta^\top a$ . However,  $\beta$  is not identifiable.

To see this, let  $\Sigma_{AA} \in \mathbb{R}^{p \times p}$  be the covariance of  $A$ ,  $\Sigma_{AY} \in \mathbb{R}^p$  be the covariance between  $A$  and  $Y$ , and  $\Sigma_{YY} \in \mathbb{R}$  be the variance of  $Y$ . By linking the population covariance matrix of the observed variables and model parameters, one can construct the following equations

$$\Sigma_{AA} = \theta\theta^\top + \text{diag}(\sigma_{A,1}^2, \dots, \sigma_{A,p}^2), \quad (\text{S2})$$

$$\Sigma_{AY} = \Sigma_{AA}\beta + \gamma\theta, \quad (\text{S3})$$

$$\Sigma_{YY} = (\beta^\top\theta + \gamma)^2 + \beta^\top \text{diag}(\sigma_{A,1}^2, \dots, \sigma_{A,p}^2)\beta + \sigma_Y^2. \quad (\text{S4})$$

In this case, (S2), (S3) and (S4) are all the equations we can use to identify the parameters. In our case,  $(A^\top, Y)^\top$  follows a multivariate normal distribution, for which the first and second moments are sufficient statistics. The first moments contain no information for identification as they are all zero.

We will show that  $\beta$  is not identifiable through equations (S2), (S3) and (S4). Equation (S2) can be used to identify  $\theta$  and  $\sigma_A = (\sigma_{A,1}^2, \dots, \sigma_{A,p}^2)^\top$ . In particular, when  $p \geq 3$ , if there exists at least three elements of  $\theta = (\theta_1, \dots, \theta_p)^\top$  that are non-zero, by Theorem 5.5 of Anderson and Rubin (1956), one can identify  $\theta$  up to sign flip and uniquely identify  $\sigma_A^2$  through equation (S2).

We then show that even if  $\theta$  is identifiable, i.e. the sign can be determined,  $\beta$  is still not identifiable. Since equation (S2) only involves  $\theta$  and  $\sigma_A$ , to identify  $(\beta^\top, \gamma, \sigma_Y^2)^\top \in \mathbb{R}^{p+2}$ , one needs to use equations (S3) and (S4). However, (S3) gives  $p$  equations and (S4) gives 1 equation, and the total number of equations is only  $p+1$ . So we can not identify the  $p+2$  dimensional parameters  $(\beta^\top, \gamma, \sigma_Y^2)^\top$  from these equations without assuming additional assumptions, and thus the causal effects cannot be identified.

There were some assumptions under which  $(\beta^\top, \gamma, \sigma_Y^2)^\top$  can be identified; for example if  $\sigma_Y^2$  is known. But this requires either we have replicates of the outcome  $Y$  or proxy of the outcome  $Y$ .

### 3 Proof of Theorem 1

We first present the identifiability results for  $\theta$  and  $\sigma_A^2$ . When  $p \geq 3$ , if there exist at least three elements of  $\theta = (\theta_1, \dots, \theta_p)^\top$  that are non-zero, by Theorem 5.5 of Anderson and Rubin (1956), one can identify  $\theta$  up to sign and uniquely identify  $\sigma_A^2$ . As there exists at least one  $\theta_j \neq 0$ ,  $1 \leq j \leq p$  such that the sign of  $\theta_j$  is known,  $\theta$  is identifiable. In other words, under condition (A1),  $\theta$  and  $\sigma_A^2$  are identifiable.

We then study the identifiability for  $\alpha$ ,  $\beta$  and  $\gamma$ . As  $A$  and  $Y$  are observed, the joint distribution of  $(A, Y)$  is identifiable. This joint distribution is uniquely determined by the distribution of  $A$  and the conditional distribution  $\text{pr}(Y = 1|A = a)$ . The distribution of  $A \sim \mathcal{N}_p(0, \Sigma_{AA})$ , where  $\Sigma_{AA} = \theta\theta^\top + \text{diag}(\sigma_{A,1}^2, \dots, \sigma_{A,p}^2)$ . Then  $\Sigma_{AA}$  is identified as  $\theta$  and  $\sigma_A^2$  are identified. Define  $Q(a) = \text{pr}(Y = 1|A = a)$ , which is identifiable for any  $a \in \mathbb{R}^p$ .

One can write

$$Q(a) = \text{pr}(Y = 1|A = a) = \int \text{pr}(Y = 1|A = a, U = u)f_{U|A}(u|a)du,$$

where  $f_{U|A}(u|a)$  is the probability density function of  $U|A$ . By model (2) and the assumptions on  $U$  and  $A$ , one can see that  $(U, A)$  is joint multivariate normal. Specifically,

$$\begin{pmatrix} U \\ A \end{pmatrix} \sim \mathcal{N}_{p+1}(0, \Sigma_J),$$

where

$$\Sigma_J = \begin{pmatrix} 1 & \theta^T \\ \theta & \Sigma_{AA} \end{pmatrix}.$$

Therefore,  $U|A = a$  is univariate normal with mean  $\mu_{U|a} = \theta^T \Sigma_{AA}^{-1} a$  and standard deviation  $\sigma_{U|a} = (1 - \theta^T \Sigma_{AA}^{-1} \theta)^{1/2}$ .

Define  $v = (u - \mu_{U|a})/\sigma_{U|a}$ , one has

$$\begin{aligned} Q(a) &= \int g(\alpha + \beta^T a + \gamma u) f_{U|A}(u|a) du \\ &= \int g\{\alpha + \beta^T a + \gamma(\sigma_{U|a} v + \mu_{U|a})\} \phi(v) dv \\ &= \int g\{\alpha + (\beta^T + \gamma \theta^T \Sigma_{AA}^{-1}) a + \gamma \sigma_{U|a} v\} \phi(v) dv, \end{aligned}$$

where  $\phi(\cdot)$  is the probability density function of standard normal.

Define  $c_1 = \alpha$ ,  $c_2 = (c_{21}, \dots, c_{2p})^T = \beta + \gamma \Sigma_{AA}^{-1} \theta$  and  $c_3 = \gamma \sigma_{U|a}$ , by condition (A1), one has  $c_3 > 0$ . We can write  $Q(a) = \int g(c_1 + c_2^T a + c_3 v) \phi(v) dv$ . The values of  $c_1$ ,  $c_2$  and  $c_3$  are determined by the function  $Q(\cdot)$ , which we show in the following proof.

We first identify  $c_{21}$ . Define  $Q_1(a^1) = \text{pr}(Y = 1|A^1 = a^1, A^2 = 0, \dots, A^p = 0) = Q(a)|_{a^2=0, \dots, a^p=0} = \int g(c_1 + c_{21} a^1 + c_3 v) \phi(v) dv$ . When  $c_{21} > 0$ , one can see that

$$\lim_{a^1 \rightarrow +\infty} Q_1(a^1) = \lim_{a^1 \rightarrow +\infty} \int g(c_1 + c_{21} a^1 + c_3 v) \phi(v) dv = \int \lim_{a^1 \rightarrow +\infty} g(c_1 + c_{21} a^1 + c_3 v) \phi(v) dv = 1.$$

Here the integration and limit are exchangeable as  $g$  and  $\phi$  are bounded. As the sigmoid function satisfies

$g' = g(1 - g)$ , one has

$$\begin{aligned}\lim_{a^1 \rightarrow +\infty} Q'_1(a^1) &= \lim_{a^1 \rightarrow +\infty} c_{21} \int g(c_1 + c_{21}a^1 + c_3v) \{1 - g(c_1 + c_{21}a^1 + c_3v)\} \phi(v) dv \\ &= c_{21} \int \lim_{a^1 \rightarrow +\infty} g(c_1 + c_{21}a^1 + c_3v) \{1 - g(c_1 + c_{21}a^1 + c_3v)\} \phi(v) dv = 0\end{aligned}$$

Here the integration and limit are exchangable as  $g$ ,  $g'$  and  $\phi$  are bounded. Therefore, one has  $\lim_{a^1 \rightarrow +\infty} Q'_1(a^1)/Q_1(a^1) = 0$ .

Next, we calculate

$$\begin{aligned}Q'_1(a^1)/Q_1(a^1) &= \frac{c_{21} \int g(c_1 + c_{21}a^1 + c_3v) \{1 - g(c_1 + c_{21}a^1 + c_3v)\} \phi(v) dv}{\int g(c_1 + c_{21}a^1 + c_3v) \phi(v) dv} \\ &= c_{21} - c_{21} \frac{\int g^2(c_1 + c_{21}a^1 + c_3v) \phi(v) dv}{\int g(c_1 + c_{21}a^1 + c_3v) \phi(v) dv}.\end{aligned}$$

As  $g(t) \leq \exp(t)$  for any  $t$ , one has

$$\int g^2(c_1 + c_{21}a^1 + c_3v) \phi(v) dv \leq \int \exp(2c_1 + 2c_{21} + 2c_3v) \phi(v) dv = \exp(2c_1 + 2c_{21} + 2c_3^2)$$

Notice that  $g(t) \geq 0.5 \exp(t)$  for any  $t < 0$ . As  $c_3 = \gamma \sigma_{U|a} \geq 0$ , for  $t < -c_1/c_{21}$ , one has

$$\begin{aligned}\int g(c_1 + c_{21}a^1 + c_3v) \phi(v) dv &\geq \int_{-\infty}^0 g(c_1 + c_{21}a^1 + c_3v) \phi(v) dv \\ &\geq 0.5 \int_{-\infty}^0 \exp(c_1 + c_{21}a^1 + c_3v) \phi(v) dv \\ &= 0.5 \exp(c_1 + c_{21}a^1) \int_{-\infty}^0 \exp(c_3v) \phi(v) dv \\ &= 0.5 \exp(c_1 + c_{21}a^1 + 0.5c_3^2) \Phi(-c_3),\end{aligned}$$

where  $\Phi(\cdot)$  is the cumulative density function of standard normal.

We can see that

$$0 \leq \lim_{a^1 \rightarrow -\infty} \frac{\int g^2(c_1 + c_{21}a^1 + c_3v) \phi(v) dv}{\int g(c_1 + c_{21}a^1 + c_3v) \phi(v) dv} \leq \lim_{a^1 \rightarrow -\infty} \frac{\exp(2c_1 + 2c_{21}a^1 + 2c_3^2)}{0.5 \exp(c_1 + c_{21}a^1 + 0.5c_3^2) \Phi(-c_3)} = 0.$$

Consequently,  $\lim_{a^1 \rightarrow -\infty} Q'_1(a^1)/Q_1(a^1) = c_{21}$ . When  $c_{21} > 0$ , one has  $\lim_{a^1 \rightarrow +\infty} Q'_1(a^1)/Q_1(a^1) = 0$  and  $\lim_{a^1 \rightarrow -\infty} Q'_1(a^1)/Q_1(a^1) = c_{21}$ .

Similarly, when  $c_{21} < 0$ , one can show that  $\lim_{a^1 \rightarrow +\infty} Q'_1(a^1)/Q_1(a^1) = c_{21}$  and  $\lim_{a^1 \rightarrow -\infty} Q'_1(a^1)/Q_1(a^1) = 0$ . When  $c_{21} = 0$ ,  $Q'_1(a^1) = 0$  for any  $a^1 \in \mathbb{R}$ , and thus  $\lim_{a^1 \rightarrow +\infty} Q'_1(a^1)/Q_1(a^1) = 0$  and  $\lim_{a^1 \rightarrow -\infty} Q'_1(a^1)/Q_1(a^1) = 0$ . Combining all the scenarios, one can identify  $c_{21}$  by  $c_{21} = \lim_{a^1 \rightarrow +\infty} Q'_1(a^1)/Q_1(a^1) + \lim_{a^1 \rightarrow -\infty} Q'_1(a^1)/Q_1(a^1)$ .

Analogously, define  $Q_j(a^j) = \text{pr}(Y = 1 | A^1 = 0, A^2 = 0, \dots, A^j = a^j, \dots, A^p = 0) =$

$Q(a)|_{a^1=0, \dots, a^{j-1}=0, a^{j+1}=0, a^p=0} = \int g(c_1 + c_{2j}a^j + c_3v)\phi(v)dv$ , one has  $c_{2j} = \lim_{a^j \rightarrow +\infty} Q'_j(a^j)/Q_j(a^j) + \lim_{a^j \rightarrow -\infty} Q'_j(a^j)/Q_j(a^j)$  for  $1 \leq j \leq p$ , and thus  $c_2$  can be identifiable.

As  $\phi(\cdot)$  is a symmetric function, one has  $\int g(c_3v)\phi(v)dv = g(0) = 0.5$ . By condition (A2), there exists  $j$  such that  $c_{2j} \neq 0$ , thus one has  $Q_j(-c_1/c_{2j}) = 0.5$ . As  $Q'_j(a^j) = c_{2j} \int g(c_1 + c_{2j}a^j + c_3v)\{1 - g(c_1 + c_{2j}a^j + c_3v)\}\phi(v)dv$ ,  $Q'_j(a^j)$  has the same sign as  $c_{2j}$ , and therefore  $Q_j(a^j)$  is strictly monotone, i.e. it is strictly increasing if  $c_{2j} > 0$  and strictly decreasing if  $c_{2j} < 0$ . Thus,  $Q_j^{-1}$  exists, and one has  $c_1 = -Q_j^{-1}(0.5)c_{2j}$ .

Define a function  $K : \mathbb{R}_0^+ \rightarrow \mathbb{R}$  by  $K(s) = \int g(1 + sv)\phi(v)dv$ , where  $\mathbb{R}_0^+$  denotes the set of all positive real numbers. We first prove that the function is strictly monotone on  $\mathbb{R}_0^+$ , and thus invertible on  $\mathbb{R}_0^+$ . To show this, we calculate the derivative of  $K(s)$  as  $K'(s) = \int g'(1 + sv)v\phi(v)dv$ .

For positive  $v$  and  $s$ , one has  $|1 + sv| > |1 - sv|$ , and therefore  $g'(1 + sv) < g'(1 - sv)$ . As  $\phi(\cdot)$  is symmetric, we have

$$\begin{aligned} \int_0^\infty g'(1 + sv)v\phi(v)dv &< \int_0^\infty g'(1 - sv)v\phi(v)dv \\ &= \int_0^{-\infty} g'(1 + sv)v\phi(v)dv \\ &= -\int_{-\infty}^0 g'(1 + sv)v\phi(v)dv. \end{aligned}$$

Consequently,  $K'(s) = \int g'(1 + sv)v\phi(v)dv = \int_0^\infty g'(1 + sv)v\phi(v)dv + \int_{-\infty}^0 g'(1 + sv)v\phi(v)dv < 0$  for all  $s > 0$ . This implies  $K(\cdot)$  is strictly monotone on  $\mathbb{R}_0^+$ , and thus invertible on  $\mathbb{R}_0^+$ . If there exists a  $c_{2j} \neq 0$ , one has  $K(c_3) = Q_j\{(1 - c_1)/c_{2j}\}$ , and therefore  $c_3 = K^{-1}[Q_j\{(1 - c_1)/c_{2j}\}]$ .

As  $c_1 = \alpha$ ,  $c_2 = (c_{21}, \dots, c_{2p})^T = \beta + \gamma \Sigma_{AA}^{-1} \theta$  and  $c_3 = \gamma \sigma_{U|a}$ , the parameters can be solved by  $\alpha = c_1$ ,  $\gamma = c_3 \sigma_{U|a}^{-1}$  and  $\beta = c_2 - \gamma \Sigma_{AA}^{-1} \theta$  by noticing that both  $\sigma_{U|a}$  and  $\Sigma_{AA}$  have already been identified through the factor model (2).

In sum,  $\alpha$ ,  $\beta$  and  $\gamma$  can be identified through the following equations,

$$\alpha = c_1, \tag{S5}$$

$$\beta = c_2 - \gamma \Sigma_{AA}^{-1} \theta, \tag{S6}$$

$$\gamma = c_3 (1 - \theta^T \Sigma_{AA}^{-1} \theta)^{1/2}, \tag{S7}$$

where  $\theta$  and  $\Sigma_{AA}^{-1}$  are identified through the factor model (2). The  $c_1, c_2 = (c_{21}, \dots, c_{2p})^T \in \mathbb{R}^p$  and  $c_3$  are identified through

$$\begin{aligned} c_{2j} &= \lim_{a^j \rightarrow +\infty} Q'_j(a^j)/Q_j(a^j) + \lim_{a^j \rightarrow -\infty} Q'_j(a^j)/Q_j(a^j) \text{ for } 1 \leq j \leq p, \\ c_1 &= -Q_j^{-1}(0.5)c_{2j}, \\ c_3 &= K^{-1}[Q_j\{(1 - c_1)/c_{2j}\}], \end{aligned}$$

for some  $c_{2j} \neq 0$ . Thus  $E\{Y(a)\} = E\{E(Y|A = a, U)\} = \int g(\alpha + \beta^T a + \gamma u)\phi(u)du$  is identifiable.

**Remark 1** If  $c_{2j} = 0$  for all  $1 \leq j \leq p$ ,  $Q(a) = \text{pr}(Y = 1)$  for any  $a$ , and we have  $\text{pr}(Y = 1) = \int g(c_1 + c_3 v)\phi(v)dv$ . In this case we can not identify  $c_1$  and  $c_3$  as we have two parameters, but only one equation. Therefore, the parameters are not identifiable.

## 4 Proof of Theorem 3

The identifiability results for  $\theta$  and  $\sigma_A^2$  are the same as that in proof of Theorem 1. In particular, under condition (A1), one can identify  $\theta$  and  $\sigma_A^2$ .

We will show under models (2) and (7),  $E\{Y(a)\}$  is not identifiable. One can write

$$\begin{aligned} Q(a) &= \int \Phi(\alpha + \beta^T a + \gamma u) f_{U|A}(u|a) du \\ &= \int \Phi\{\alpha + \beta^T a + \gamma(\sigma_{U|a} v + \mu_{U|a})\} \phi(v) dv \\ &= \int \Phi\{\alpha + (\beta^T + \gamma \theta^T \Sigma_{AA}^{-1}) a + \gamma \sigma_{U|a} v\} \phi(v) dv, \end{aligned}$$

where  $\phi(\cdot)$  is the probability density function of standard normal.

Define  $c_1 = \alpha$ ,  $c_2 = (c_{21}, \dots, c_{2p})^T = \beta + \gamma \Sigma_{AA}^{-1} \theta$  and  $c_3 = \gamma \sigma_{U|a}$ , one can write

$$\begin{aligned} Q(a) &= \int \Phi(c_1 + c_2^T a + c_3 v) \phi(v) dv \\ &= \int_{-\infty}^{\infty} \int_{-\infty}^{c_1 + c_2^T a + c_3 v} \phi(u) du \phi(v) dv \\ &= \text{pr}(Z_1 < c_1 + c_2^T a + c_3 Z_2) \\ &= \text{pr}(Z_1 - c_3 Z_2 < c_1 + c_2^T a) \\ &= \Phi\{(c_1 + c_2^T a)(1 + c_3^2)^{-1/2}\}, \end{aligned}$$

where  $Z_1$  and  $Z_2$  are two independent standard normal random variables.

One can see  $Y|A$  follows a probit model with intercept  $c_1(1 + c_3^2)^{-1/2}$  and regression slopes  $(1 + c_3^2)^{-1/2}c_2$ , and therefore  $c_1(1 + c_3^2)^{-1/2}$  and  $(1 + c_3^2)^{-1/2}c_2$  are identifiable by  $Q(a)$ , say  $c_1(1 + c_3^2)^{-1/2} = k_1 \in \mathbb{R}$  and  $(1 + c_3^2)^{-1/2}c_2 = k_2 \in \mathbb{R}^p$ . Meanwhile the values  $k_1$  and  $k_2$  uniquely determine  $Q(a)$ . Therefore, for any  $(c_1, c_2^T, c_3)^T$ , as long as they satisfy  $c_1(1 + c_3^2)^{-1/2} = k_1$  and  $(1 + c_3^2)^{-1/2}c_2 = k_2$ , they are the solutions. One can easily see there are infinite solutions, and therefore  $(c_1, c_2^T, c_3)^T$  is not identifiable. As  $\alpha = c_1$ ,  $\gamma = c_3(1 - \theta^T \Sigma_{AA}^{-1} \theta)^{1/2}$  and  $\beta = c_2 - \gamma \Sigma_{AA}^{-1} \theta$ , one can see  $\alpha$ ,  $\beta$  and  $\gamma$  have infinite solutions and are not identifiable.

We will then show that there exist two sets of solutions  $(\alpha, \beta^T, \gamma)^T$  such that  $E\{Y(a)\} = E\{E(Y|A = a, U)\} = \int \Phi(\alpha + \beta^T a + \gamma u)\phi(u)du = \Phi\{(\alpha + \beta^T a)(1 + \gamma^2)^{-1/2}\}$  have different values.



As  $c_1(1 + c_3^2)^{-1/2} = k_1$  and  $(1 + c_3^2)^{-1/2}c_2 = k_2$ , one solution for  $(c_1, c_2^T, c_3)^T$  is  $(k_1, k_2^T, 0)^T$ . We then obtain  $\alpha = k_1$ ,  $\beta = k_2$  and  $\gamma = 0$ , and the mean potential outcome  $E\{Y(a)\} = \Phi(k_1 + k_2^T a)$ . Another solution for  $(c_1, c_2^T, c_3)^T$  is  $(2k_1, 2k_2^T, \sqrt{3})^T$ . We can obtain  $\alpha = 2k_1$ ,  $\beta = 2k_2 - \sqrt{3}(1 - \theta^T \Sigma_{AA}^{-1} \theta)^{1/2} \Sigma_{AA}^{-1} \theta$  and  $\gamma = \sqrt{3}(1 - \theta^T \Sigma_{AA}^{-1} \theta)^{1/2}$ . In this case, the mean potential outcome  $E\{Y(a)\} = \Phi\{[2k_1 + \{2k_2 - \sqrt{3}(1 - \theta^T \Sigma_{AA}^{-1} \theta)^{1/2} \Sigma_{AA}^{-1} \theta\}^T a](4 - 3\theta^T \Sigma_{AA}^{-1} \theta)^{-1/2}\}$ . One can see two sets of solutions for  $(c_1, c_2^T, c_3)^T$  give two different mean potential outcomes, and thus  $E\{Y(a)\}$  is not identifiable.

## 5 Data Usage Acknowledgement

Data used in preparation of this article were obtained from the Alzheimer’s Disease Neuroimaging Initiative (ADNI) database ([adni.loni.usc.edu](http://adni.loni.usc.edu)). As such, the investigators within the ADNI contributed to the design and implementation of ADNI and/or provided data but did not participate in analysis or writing of this report. A complete listing of ADNI investigators can be found at: [http://adni.loni.usc.edu/wp-content/uploads/how\\_to\\_apply/ADNI\\_Acknowledgement\\_List.pdf](http://adni.loni.usc.edu/wp-content/uploads/how_to_apply/ADNI_Acknowledgement_List.pdf)

Data used in the preparation of this article were obtained from the Alzheimer’s Disease Neuroimaging Initiative (ADNI) database ([adni.loni.usc.edu](http://adni.loni.usc.edu)). The ADNI was launched in 2003 as a public-private partnership, led by Principal Investigator Michael W. Weiner, MD. The primary goal of ADNI has been to test whether serial magnetic resonance imaging (MRI), positron emission tomography (PET), other biological markers, and clinical and neuropsychological assessment can be combined to measure the progression of mild cognitive impairment (MCI) and early Alzheimer’s disease (AD). For up-to-date information, see [www.adni-info.org](http://www.adni-info.org).

Data collection and sharing for this project was funded by the Alzheimer’s Disease Neuroimaging Initiative (ADNI) (National Institutes of Health Grant U01 AG024904) and DOD ADNI (Department of Defense award number W81XWH-12-2-0012). ADNI is funded by the National Institute on Aging, the National Institute of Biomedical Imaging and Bioengineering, and through generous contributions from the following: AbbVie, Alzheimer’s Association; Alzheimer’s Drug Discovery Foundation; Araclon Biotech; BioClinica, Inc.; Biogen; Bristol-Myers Squibb Company; CereSpir, Inc.; Cogstate; Eisai Inc.; Elan Pharmaceuticals, Inc.; Eli Lilly and Company; EuroImmun; F. Hoffmann-La Roche Ltd and its affiliated company Genentech, Inc.; Fujirebio; GE Healthcare; IXICO Ltd.; Janssen Alzheimer Immunotherapy Research & Development, LLC.; Johnson & Johnson Pharmaceutical Research & Development LLC.; Lumosity; Lundbeck; Merck & Co., Inc.; Meso Scale Diagnostics, LLC.; NeuroRx Research; Neurotrack Technologies; Novartis Pharmaceuticals Corporation; Pfizer Inc.; Piramal Imaging; Servier; Takeda Pharmaceutical Company; and Transition Therapeutics. The Canadian Institutes of Health Research is providing funds to support ADNI clinical sites in Canada. Private sector contributions are facilitated by the Foundation for the National Institutes of Health ([www.fnih.org](http://www.fnih.org)). The grantee organization is the Northern California Institute for Research and Education, and the study is coordinated by the Alzheimer’s Therapeutic Research Institute at the University of Southern California. ADNI data are disseminated by the Laboratory for Neuro Imaging at the University of Southern California.